PNAS
www.pnas.org

Supporting Information

Structural basis of peptidomimetic agonism revealed by small-molecule GLP-1R agonists Boc5 and WB4-24

Zhaotong Cong[a,1], Qingtong Zhou[a,1], Yang Li[a], Li-Nan Chen[b,c], Zi-Chen Zhang[d], Anyi Liang[e], Qing Liu[f], Xiaoyan Wu[f], Antao Dai[f], Tian Xia[e], Wei Wu[d], Yan Zhang[b,c], Dehua Yang[f,g,h,i,2], Ming-Wei Wang[a,f,g,h,i,j,2]

[a]Department of Pharmacology, School of Basic Medical Sciences, Fudan University, Shanghai 200032, China; [b]Department of Biophysics of Sir Run Run Shaw Hospital, Zhejiang University School of Medicine, Hangzhou 310058, China; [c]Department of Pathology of Sir Run Run Shaw Hospital, Zhejiang University School of Medicine, Hangzhou 310058, China; [d]School of Pharmacy, Fudan University, Shanghai 201203, China; [e]School of Artificial Intelligence and Automation, Huazhong University of Science and Technology, Wuhan 430074, China; [f]The National Center for Drug Screening, Shanghai Institute of Materia Medica, Chinese Academy of Sciences, Shanghai 201203, China; [g] School of Graduate Studies, University of Chinese Academy of Sciences, Beijing 100049, China; [h]The CAS Key Laboratory of Receptor Research, Shanghai Institute of Materia Medica, Chinese Academy of Sciences, Shanghai 201203, China; [i]Department of Bioactivity Screening, Research Center for Deepsea Bioresources, Sanya, Hainan 572025, China; [j]Department of Chemistry, School of Science, The University of Tokyo, Tokyo 113-0033, Japan.

[1]Z.C. and Q.Z. contributed equally to this work.

[2]To whom correspondence may be addressed: dhyang@simm.ac.cn or mwwang@simm.ac.cn

This PDF file includes:

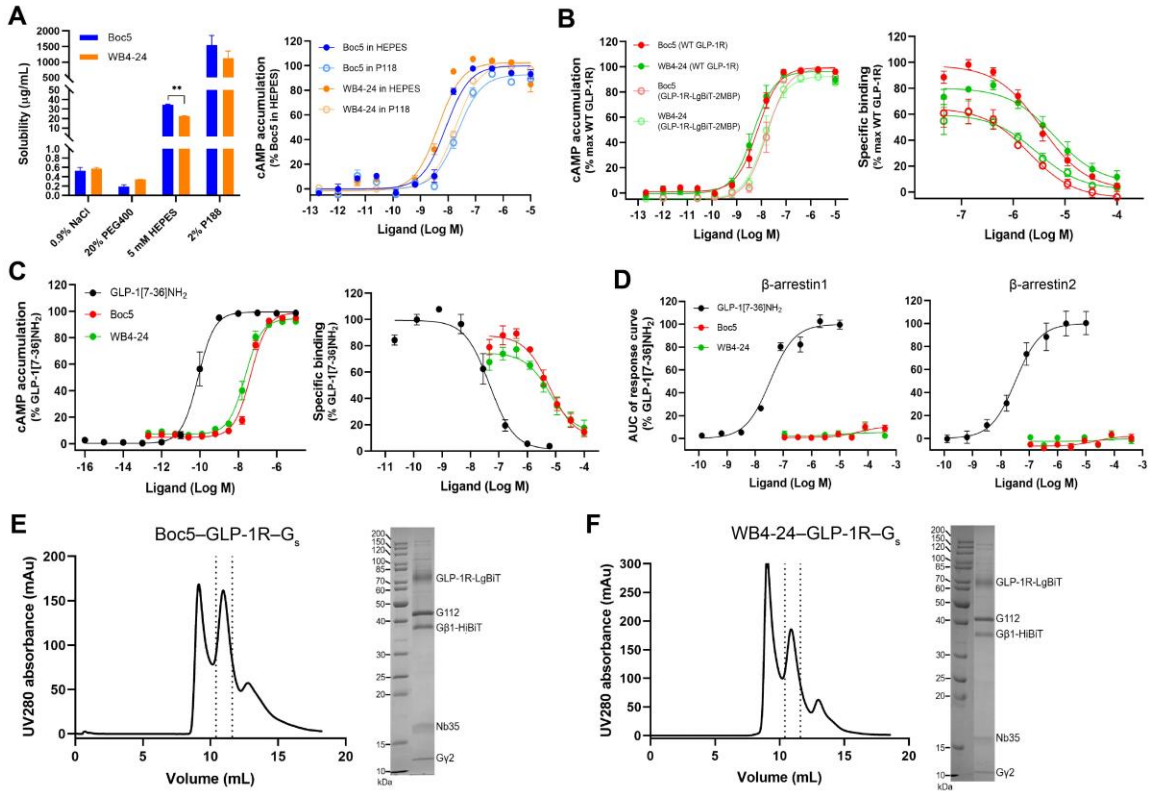

Fig. S1. Characterization of non-peptidic GLP-1R agonists and purification of Boc5- and WB4-24-bound GLP-1R–G_s complexes. (***A***) Solubility of Boc5 and WB4-24 in different solvents (left). The surfactant P188 had no significant influence on Boc5 and WB4-24 induced receptor activation (right). (***B***) cAMP responses following Boc5 and WB4-24 stimulation in HEK293T cells transfected with the wild-type (WT) or modified GLP-1R constructs (left). Binding of Boc5 and WB4-24 to the WT or modified GLP-1R in competition with ^{125}I-GLP-1 (right). (***C***, ***D***) GLP-1, Boc5 and WB4-24 induced cAMP accumulation (***C***) and β-arrestin 1/2 recruitment (***D***). The color key at the upper left corner provides ligand information for each assay. (***E***, ***F***) Size-exclusion chromatography elution profile and corresponding SDS-PAGE gel of the Boc5–GLP-1R–G_s–Nb35 (***E***) and WB4-24–GLP-1R–G_s–Nb35 (***F***) complexes. G112 is an engineered $G\alpha_s$ protein. Data are shown as means ± SEM from at least three independent experiments.

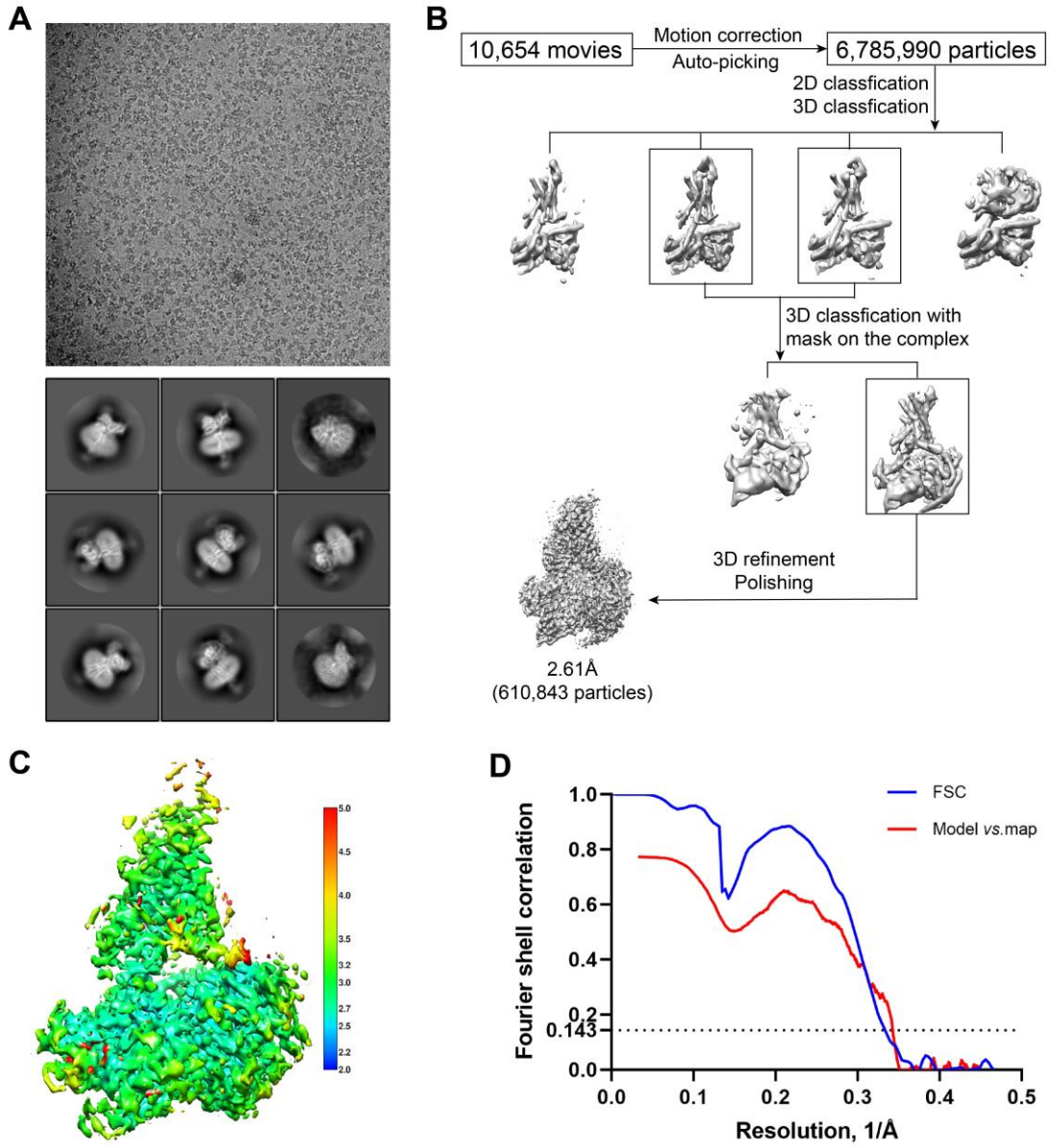

Fig. S2. Cryo-EM data processing and validation of the Boc5–GLP-1R–G_s–Nb35 complex. (***A***) Representative cryo-EM micrograph and two-dimensional class averages. (***B***) Flow chart of cryo-EM data processing. (***C***) Local resolution distribution map of the complex. (***D***) Fourier shell correlation (FSC) curve of the overall refined receptor.

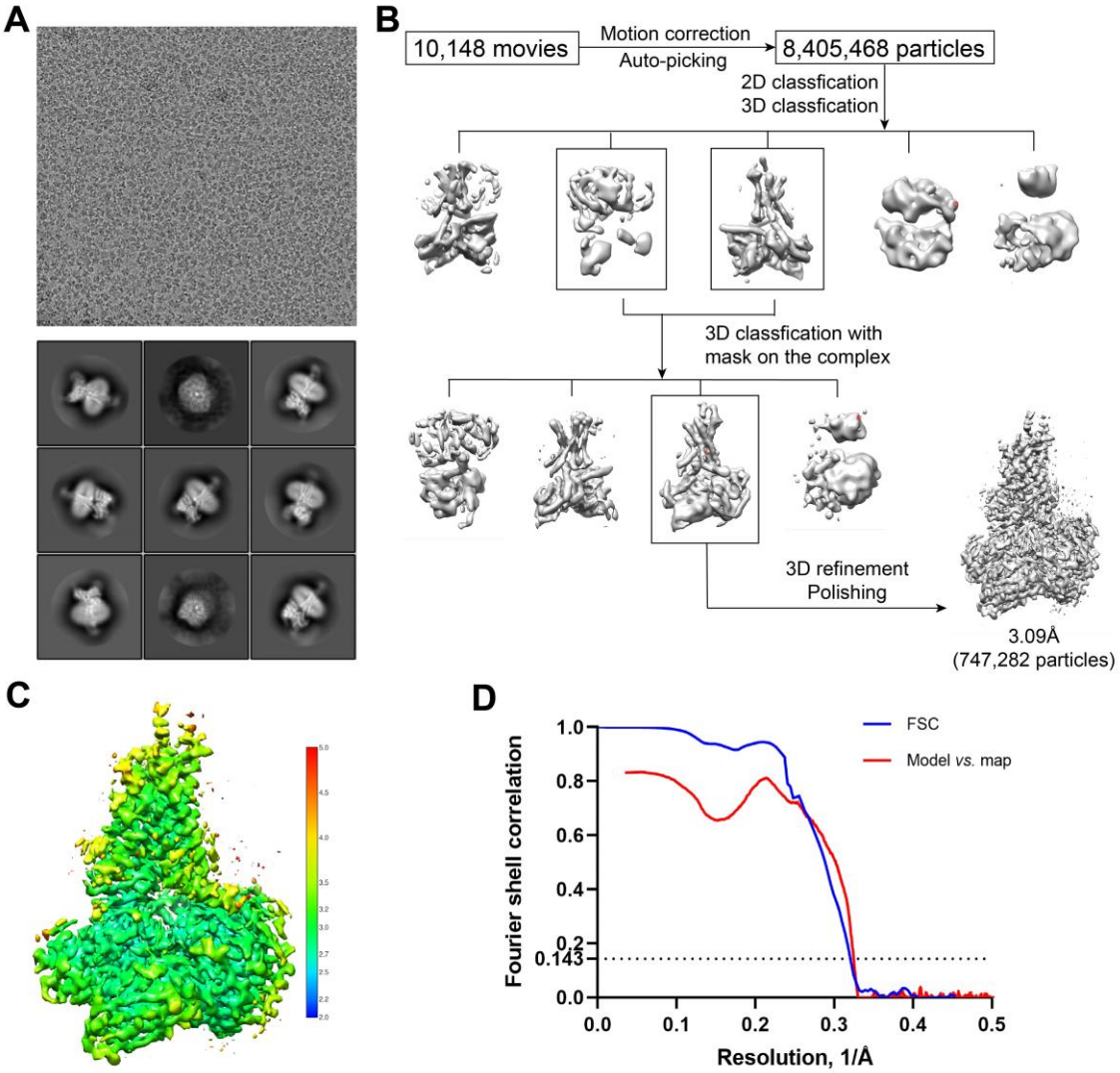

Fig. S3. Cryo-EM data processing and validation of the WB4-24–GLP-1R–G_s–Nb35 complex. (***A***) Representative cryo-EM micrograph and two-dimensional class averages. (***B***) Flow chart of cryo-EM data processing. (***C***) Local resolution distribution map of the complex. (***D***) FSC curves of the overall refined receptor.

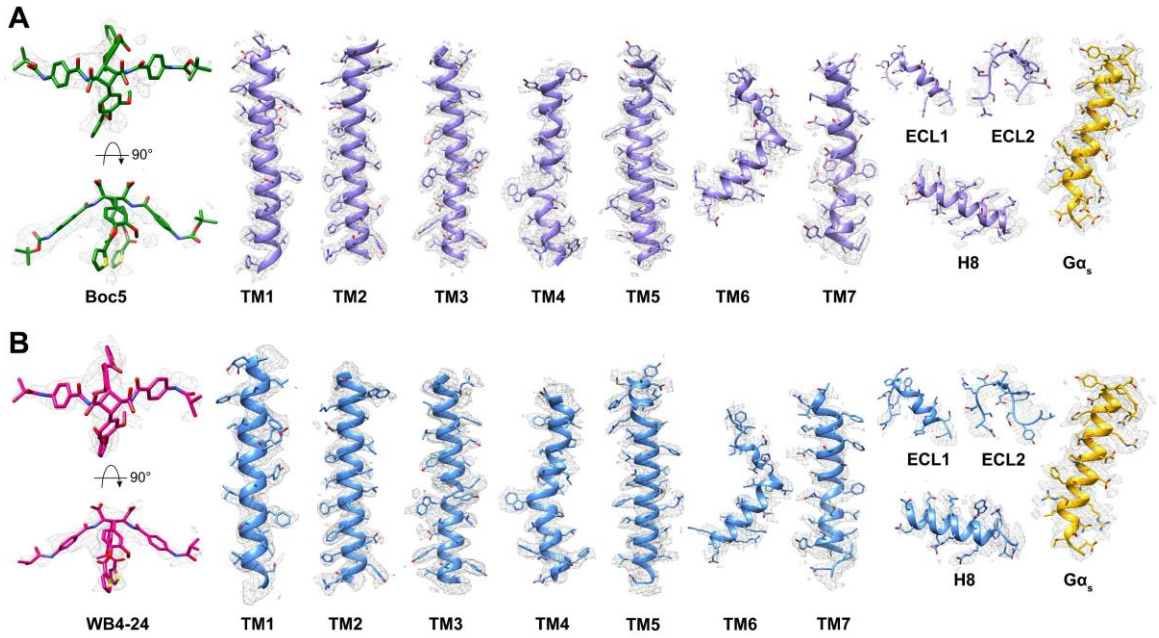

Fig. S4. Cryo-EM density maps of the Boc5- and WB4-24-bound GLP-1R–G_s structures. (***A***) Cryo-EM density map and model of the Boc5–GLP-1R–G_s structure are shown for Boc5, all seven-transmembrane (TM) α-helices, ECL1, ECL2, helix 8 (H8) of GLP-1R, and α5-helix of $Gα_s$. (***B***) Cryo-EM density map and model of the WB4-24–GLP-1R–G_s structure are shown for WB4-24, all TM α-helices, ECL1, ECL2, H8 of GLP-1R, and α5-helix of $Gα_s$.

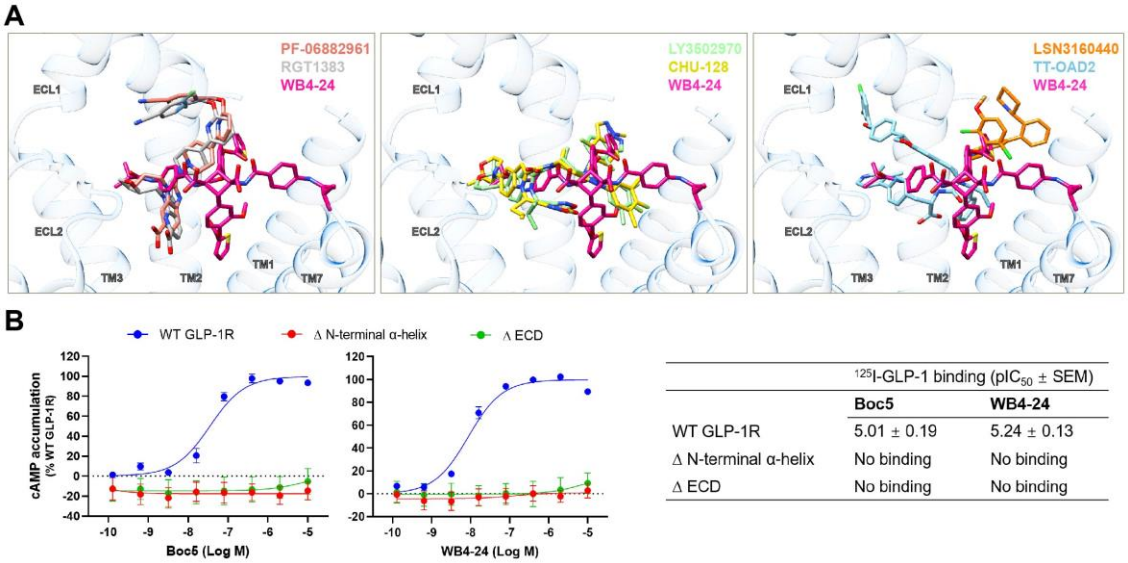

	^{125}I-GLP-1 binding (pIC$_{50}$ ± SEM)	
	Boc5	**WB4-24**
WT GLP-1R	5.01 ± 0.19	5.24 ± 0.13
Δ N-terminal α-helix	No binding	No binding
Δ ECD	No binding	No binding

Fig. S5. Comparison of binding modes of WB4-24 and other small-molecule GLP-1R agonists. (***A***) All structures were overlay with that of WB4-24-bound GLP-1R colored in blue. Each ligand is shown with different color (WB4-24, magenta; PF-06882961, salmon; RGT1383, gray; LY3502970, light green; CHU-128, yellow; TT-OAD2, sky blue; and LSN3160440, orange red). (***B***) Signaling profiles of Boc5 and WB4-24 at GLP-1R with the N-terminal α-helix or ECD truncation. Boc5 and WB4-24 concentration-response curves were derived from cAMP production assay. Binding data were normalized to the maximal binding of ^{125}I-GLP-1 and shown as pIC$_{50}$ (the negative logarithm of binding affinity). Data are shown as means ± SEM of at least four independent experiments performed in quadruplicate. WT, wild-type; Δ, truncation.

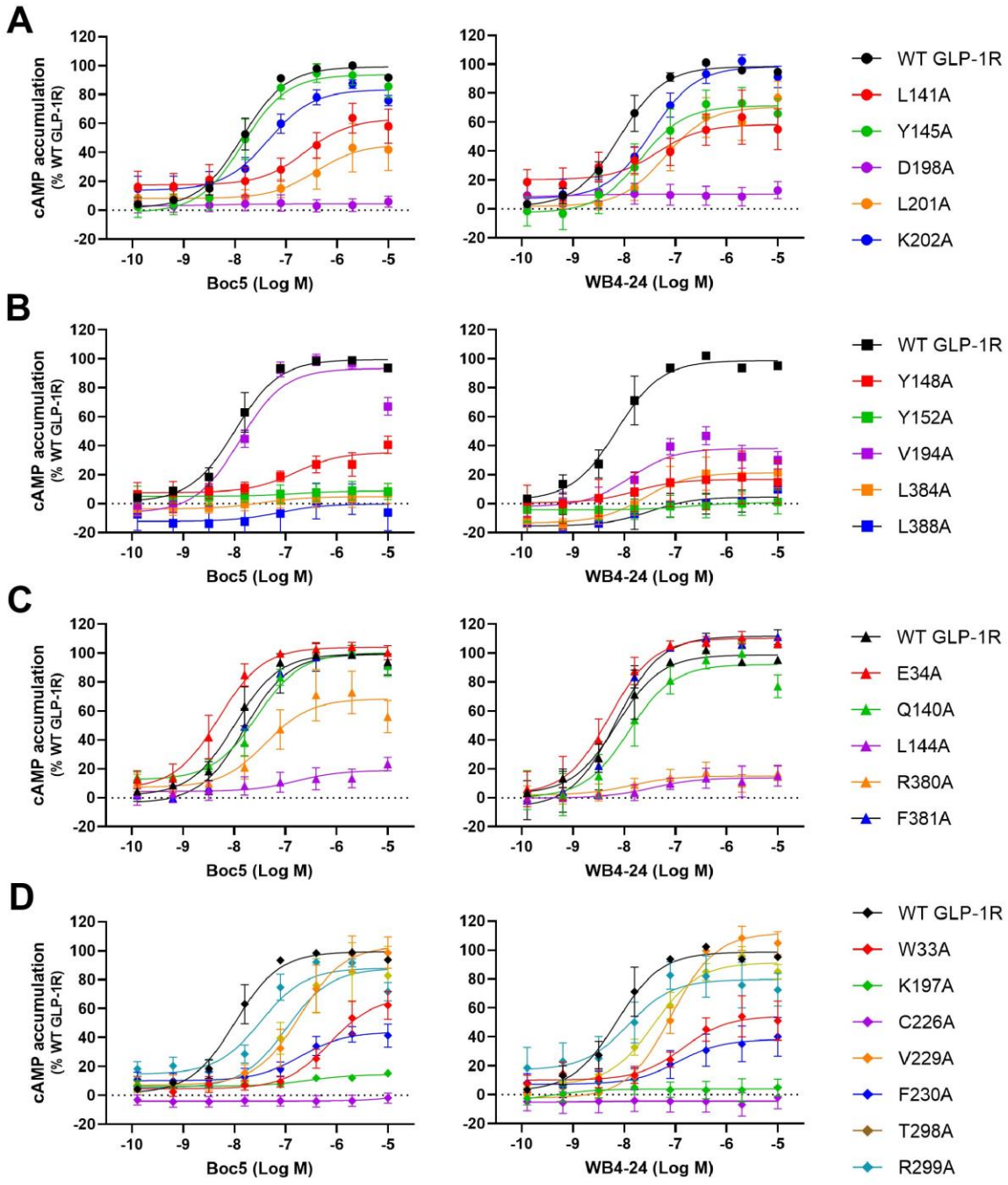

Fig. S6. Ligand mediated cAMP accumulation at wild-type (WT) or mutant GLP-1R. Concentration-response curves for alanine mutation of residues interacting with arms A1-1 (***A***), A1-2 (***B***), B1-1 or B2-1 (***C***), and B2-1 or B2-2 (***D***) of Boc5 and WB4-24. Data are shown as means ± SEM of at least four independent experiments performed in quadruplicate.

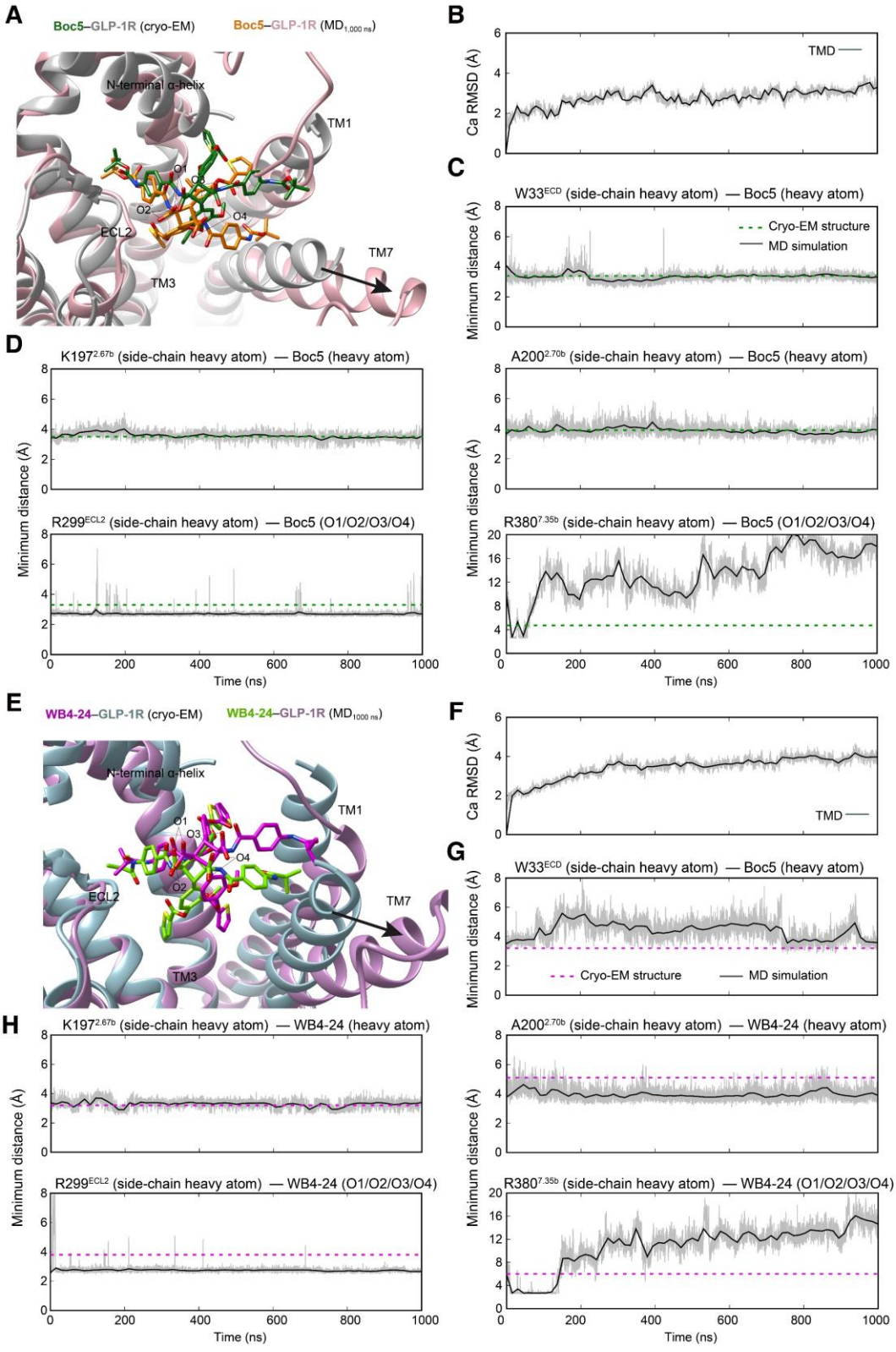
A
Boc5–GLP-1R (cryo-EM)
Boc5–GLP-1R (MD1,000 ns)
N-terminal α-helix
TM1
O1
O3
O2
O4
ECL2
TM7
TM3
B
Ca RMSD (Å)
TMD
C
W33ECD (side-chain heavy atom) — Boc5 (heavy atom)
Minimum distance (Å)
Cryo-EM structure
MD simulation
D
K1972.67b (side-chain heavy atom) — Boc5 (heavy atom)
R299ECL2 (side-chain heavy atom) — Boc5 (O1/O2/O3/O4)
A2002.70b (side-chain heavy atom) — Boc5 (heavy atom)
R3807.35b (side-chain heavy atom) — Boc5 (O1/O2/O3/O4)
Time (ns)
E
WB4-24–GLP-1R (cryo-EM)
WB4-24–GLP-1R (MD1000 ns)
F
G
H
K1972.67b (side-chain heavy atom) — WB4-24 (heavy atom)
R299ECL2 (side-chain heavy atom) — WB4-24 (O1/O2/O3/O4)
A2002.70b (side-chain heavy atom) — WB4-24 (heavy atom)
R3807.35b (side-chain heavy atom) — WB4-24 (O1/O2/O3/O4)

Fig. S7. Molecular dynamics (MD) simulations of Boc5 or WB4-24-bound active GLP-1R. (***A***) Comparison of the Boc5 conformation between simulation snapshot and the cryo-EM structure. (***B***) Root mean square deviation (RMSD) of Cα positions of the GLP-1R TMD, where all snapshots were superimposed on the cryo-EM structure of Boc5-bound GLP-1R TMD using the Cα atoms. (***C***) Minimum distance between the heavy atoms of Boc5 and the ECD residue W33 suggests that Boc5 steadily interacts with the N-terminal α-helix of ECD. (***D***) Analysis of the MD simulation trajectories in (***A***): representative minimum distances between the heavy atoms of Boc5 and TMD residues (top left, $K197^{2.67b}$—Boc5; top right, $A200^{2.70b}$—Boc5; bottom left, $R299^{ECL2}$—O1/O2/O3/O4 in Boc5; bottom right, $R380^{7.45b}$—O1/O2/O3/O4 in Boc5). (***E***) Comparison of the WB4-24 conformation between simulation snapshot and the cryo-EM structure. (***F***) RMSD of Cα positions of the GLP-1R TMD, where all snapshots were superimposed on the cryo-EM structure of WB4-24-bound GLP-1R TMD using the Cα atoms. (***G***) Minimum distance between the heavy atoms of WB4-24 and the ECD residue W33. (***H***) Analysis of the MD simulation trajectories in (***E***): representative minimum distances between the heavy atoms of WB4-24 and TMD residues (top left, $K197^{2.67b}$—WB4-24; top right, $A200^{2.70b}$—WB4-24; bottom left, $R299^{ECL2}$—O1/O2/O3/O4 in WB4-24; bottom right, $R380^{7.45b}$—O1/O2/O3/O4 in WB4-24). The thick and thin traces represent moving averages and original, unsmoothed values, respectively.

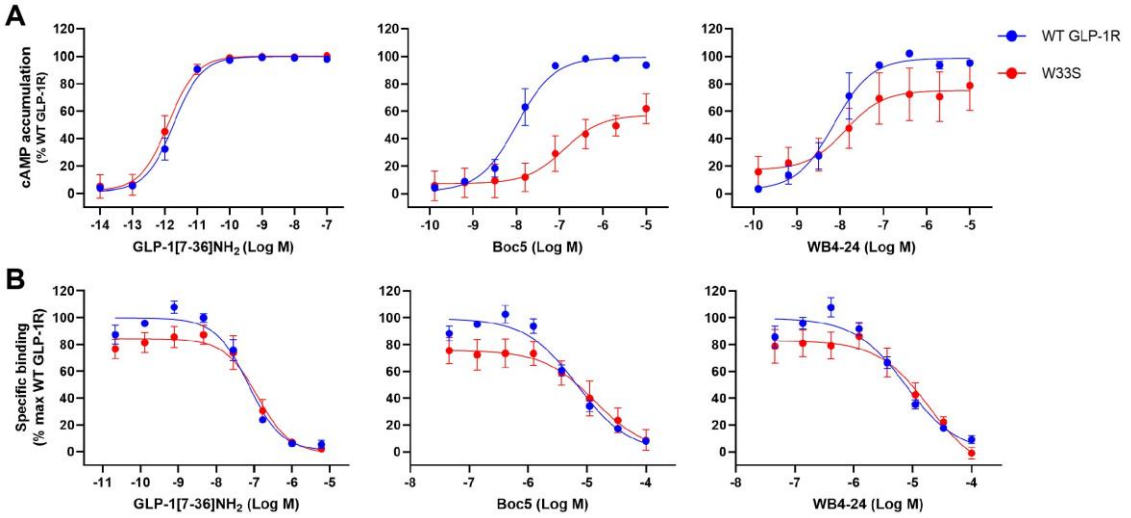

Fig. S8. Signaling profiles of GLP-1, Boc5, and WB4-24 at W33S mutant. (***A***) cAMP accumulation induced by GLP-1, Boc5 and WB4-24 at wild-type (WT) and mutant GLP-1Rs. (***B***) Specific binding of GLP-1, Boc5 and WB4-24 to the WT and mutant GLP-1Rs in competition with ^{125}I-GLP-1. Data are shown as means ± SEM from at least three independent experiments.

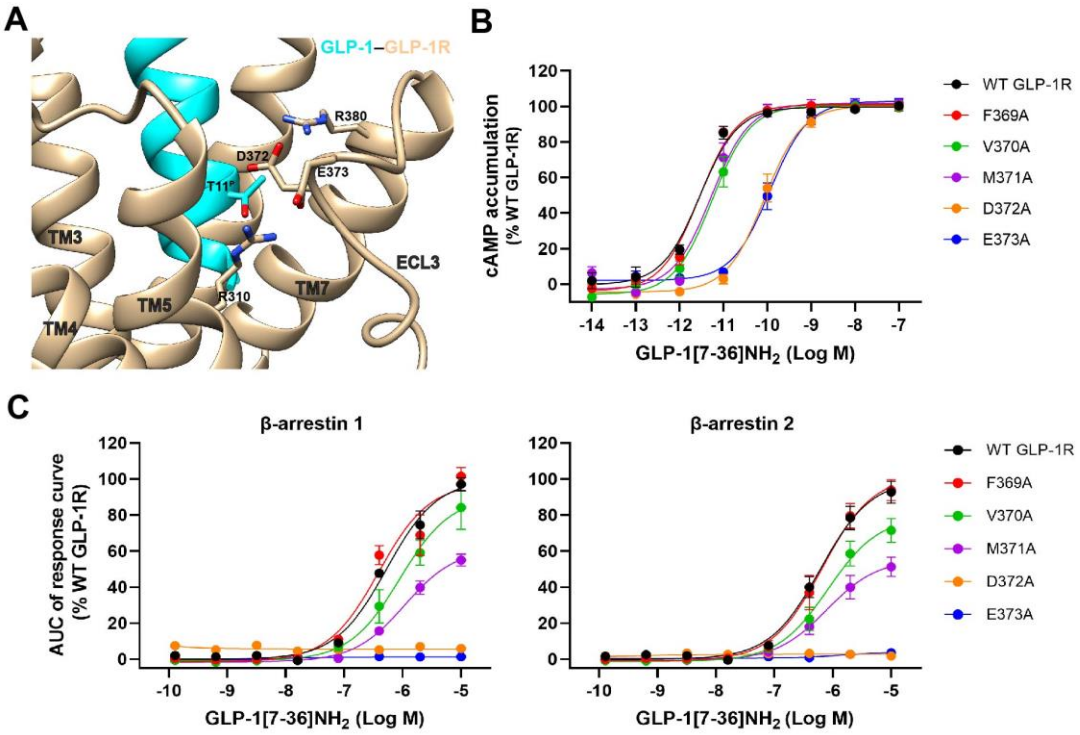

Fig. S9. ECL3 conformation is important for biased signaling at GLP-1R. In the GLP-1-bound structure (PDB code: 6X18), ECL3 is stablized by the intra-receptor interactions among R310$^{5.40b}$, D372^{ECL3}, E373^{ECL3} and R380$^{7.35b}$, as well as that between ligand and receptor inlcuding D372^{ECL3} and T11^{P} (***A***). Alanine mutations of D372^{ECL3} and E373^{ECL3} made negligible influence on the maximal response of cAMP accumulation (***B***), but completely abolished the β-arrestin 1/2 recruitment (***C***). Data are shown as means ± SEM of at least four independent experiments performed in quadruplicate. WT, wild-type.

Table S1. Cryo-EM data collection, model refinement and validation statistics.

Data collection and processing	**Boc5─GLP-1R─G_s─Nb35**	**WB4-24─GLP-1R─G_s─Nb35**
Magnification	130,000	130,000
Voltage (kV)	300	300
Electron exposure (e–/Å^2)	80	80
Defocus range (μm)	-1.2 to -2.2	-1.2 to -2.2
Pixel size (Å)	1.071	1.071
Symmetry imposed	C1	C1
Initial particle image (no.)	6,785,990	8,405,468
Final particle image (no.)	610,843	747,282
Map resolution (Å)	2.61	3.09
FSC threshold	0.143	0.143
Map resolution range (Å)	2.5-4.9	2.2-4.0
Refinement		
Initial model used (PDB code)	6X19	6X19
Model resolution (Å)	2.7	3.03
FSC threshold	0.5	0.5
Map sharpening B factor (Å^2)	-82.56	-82.56
Model composition		
Non-hydrogen atom	8,493	8,047
Protein residue	1,051	1,019
B factors (Å^2)		
Protein	46.54	93.64
Root mean square deviation		
Bond length (Å)	0.003	0.004
Bond angle (°)	0.642	0.679
Validation		
MolProbity score	1.59	1.39
Clash score	7.32	3.50
Poor rotamer (%)	0.11	0.0
Ramachandran plot		
Favored (%)	96.90	96.31
Allowed (%)	3.10	3.69
Disallowed (%)	0.0	0.0

Table S2. *In vitro* pharmacology of GLP-1, Boc5 and WB4-24 at wild-type and mutant GLP-1R constructs.

	cAMP		**Binding**	**β-arrestin 1**		**β-arrestin 2**	
	pEC_{50}	E_{max}	pKi	pEC_{50}	E_{max}	pEC_{50}	E_{max}
WT GLP-1R							
GLP-1	10.09 ± 0.06	99.53 ± 1.67	7.44 ± 0.14	7.47 ± 0.09	100 ± 3.01	7.48 ± 0.14	100 ± 4.71
Boc5	7.35 ± 0.05	99.06 ± 1.86	5.50 ± 0.11	4.30 ± 0.41	10.91 ± 2.78	4.64 ± 0.49	2.76 ± 2.54
WB4-24	7.64 ± 0.05	94.47 ± 1.67	5.40 ± 0.12	5.02 ± 1.56	5.26 ± 2.56	NA	NA
GLP-1R-LgBiT-2MBP							
GLP-1	ND	ND	ND	ND	ND	ND	ND
Boc5	7.78 ± 0.07	98.94 ± 2.63	5.99 ± 0.11	ND	ND	ND	ND
WB4-24	7.87 ± 0.08	92.59 ± 2.75	6.00 ± 0.09	ND	ND	ND	ND

The functional potency (EC_{50}) and (E_{max}) values for cAMP accumulation and β-arrestin recruitment assays were analyzed using a three-parameter logistic equation. pEC_{50} is the negative logarithm of the molar concentration of agonist that induced half the maximal response. E_{max} is expressed as a percentage of the response induced by GLP-1. Binding data were analyzed using a three-parameter logistic equation and normalized to the maximal binding of ^{125}I-GLP-1. pKi is the negative logarithm of peptide affinity. All values are means ± SEM of at least three independent experiments conducted in quadruplicate (cAMP accumulation) or duplicate (binding assay and β-arrestin recruitment). WT, wild-type; ND, not determined; NA, not active.

Table S3. Effects of residue mutation in the ligand binding pocket on cAMP accumulation.

GLP-1R residue	Boc5		WB4-24	
	pEC_{50}	E_{max}	pEC_{50}	E_{max}
Interaction with A-1				
WT GLP-1R	7.86 ± 0.09	99.28 ± 2.63	8.08 ± 0.10	98.57 ± 2.92
$L141^{1.36b}A$	6.63 ± 0.39**	63.12 ± 8.05**	7.34 ± 0.54**	58.35 ± 7.23**
$Y145^{1.40b}A$	7.84 ± 0.16	93.75 ± 4.12	7.68 ± 0.29*	71.41 ± 7.01**
$D198^{2.68b}A$	NA**	4.43 ± 2.33**	NA**	10.28 ± 2.97**
$L201^{2.71b}A$	6.42 ± 0.49**	45.48 ± 8.98**	7.20 ± 0.25**	70.63 ± 6.68**
$K202^{2.72b}A$	7.34 ± 0.17*	83.63 ± 4.25*	7.47 ± 0.15*	98.52 ± 4.88
Interaction with A-2				
$Y148^{1.43b}A$	6.81 ± 0.41**	35.29 ± 4.82**	NA**	16.66 ± 7.94**
$Y152^{1.47b}A$	6.82 ± 2.86**	8.66 ± 4.22**	NA**	0.69 ± 6.41**
$V194^{2.64b}A$	7.98 ± 0.15	93.34 ± 4.31	7.88 ± 0.31	38.04 ± 3.82**
$L384^{7.39b}A$	7.47 ± 1.06*	4.85 ± 3.17**	7.67 ± 0.45*	21.24 ± 5.30**
$L388^{7.43b}A$	7.12 ± 1.76	0.28 ± 8.16**	7.49 ± 0.71	4.64 ± 4.93**
Interaction with B1-1 or B2-1				
$E34^{ECD}A$	8.30 ± 0.10*	104.02 ± 3.78	8.28 ± 0.16	110.06 ± 4.67
$Q140^{1.35b}A$	7.55 ± 0.12	100.29 ± 3.42	7.91 ± 0.24	92.05 ± 6.35
$L144^{1.39b}A$	6.78 ± 0.81**	18.97 ± 5.12**	7.44 ± 0.73	13.68 ± 3.50**
$R380^{7.35b}A$	7.38 ± 0.33*	68.18 ± 7.12**	7.87 ± 0.76	15.01 ± 3.12**
$F381^{7.36b}A$	7.80 ± 0.14	99.14 ± 4.66	8.16 ± 0.15	111.53 ± 5.04
Interaction with B1-2 or B2-2				
$W33^{ECD}A$	6.13 ± 0.21**	67.98 ± 7.52**	6.39 ± 0.40**	54.48 ± 6.48**
$K197^{2.67b}A$	6.55 ± 0.47**	14.59 ± 1.82**	NA**	3.95 ± 2.42**
$C226^{3.29b}A$	NA**	3.73 ± 2.46**	NA**	NA**
$V229^{3.32b}A$	6.71 ± 0.19**	103.60 ± 8.02	7.34 ± 0.18**	111.90 ± 4.27
$F230^{3.33b}A$	6.71 ± 0.32**	43.74 ± 4.70**	6.96 ± 0.58**	38.29 ± 7.02**
$T298^{ECL2}A$	7.48 ± 0.18*	87.94 ± 4.55*	7.92 ± 0.38	79.69 ± 7.24**
$R299^{ECL2}A$	6.98 ± 0.27**	87.81 ± 9.09	7.54 ± 0.18*	91.23 ± 3.49

cAMP accumulation data were analyzed using a three-parameter logistic equation to determine pEC_{50} and E_{max} values. pEC_{50} is the negative logarithm of the molar concentration of agonist that induced half the maximal response. E_{max} for mutants is expressed as a percentage of the response induced by the wild-type (WT) GLP-1R. All values are means ± SEM of at least three independent experiments conducted in quadruplicate. One-way ANOVA was used to determine statistical significance (**P<0.01, *P<0.05). NA, not active.

Table S4. Interaction between GLP-1R and Boc5 or WB4-24.

GLP-1R residue	Boc5	WB4-24
W33^{ECD}	Stacking interaction	Stacking interaction
Q140$^{1.35b}$	Hydrophobic contacts	Hydrophobic contacts
L141$^{1.36b}$	Hydrophobic contacts	Hydrophobic contacts
L144$^{1.39b}$	Hydrophobic contacts	Hydrophobic contacts
Y145$^{1.40b}$	Stacking interaction	Stacking interaction
Y148$^{1.43b}$	Hydrophobic contacts	Hydrophobic contacts
Y152$^{1.47b}$	Hydrophobic contacts	Hydrophobic contacts
R190$^{2.60b}$	Stacking interaction	Stacking interaction
V194$^{2.64b}$	Hydrophobic contacts	Hydrophobic contacts
I196$^{2.66b}$	Hydrophobic contacts	
K197$^{2.67b}$	Stacking interaction Hydrophobic contacts	Stacking interaction Hydrophobic contacts
D198$^{2.68b}$		Hydrophobic contacts
A200$^{2.70b}$	Hydrophobic contacts	
L201$^{2.71b}$	Hydrophobic contacts	Hydrophobic contacts
K202$^{2.72b}$	Hydrophobic contacts	Hydrophobic contacts
C226$^{3.29b}$	Hydrophobic contacts	Hydrophobic contacts
V229$^{3.32b}$	Hydrophobic contacts	Hydrophobic contacts
F230$^{3.33b}$	Stacking interaction	Stacking interaction
M233$^{3.36b}$	Hydrophobic contacts	
T298^{ECL2}	Hydrogen bond	Hydrogen bond
R299^{ECL2}	Salt bridge	Salt bridge
R380$^{7.35b}$	Salt bridge	Salt bridge
F381$^{7.36b}$	Hydrophobic contacts	Hydrophobic contacts
L384$^{7.39b}$	Hydrophobic contacts	Hydrophobic contacts
F385$^{7.40b}$		Hydrophobic contacts
L388$^{7.43b}$	Hydrophobic contacts	Hydrophobic contacts

Table S5. Comparison of in vivo and in vitro activities of peptidic and non-peptidic GLP-1R agonists.

Ligand	Peptide	Small molecule				
	GLP-1	**Boc5**	**WB4-24**	**TT-OAD2**	**LY3502970**	**PF-06882961**
In vitro activity						
cAMP response	Full agonist	Full agonist	Full agonist	Partial agonist	Partial agonist	Full agonist
β-arrestin recruitment	Full agonist	NA	NA	NA	NA	Partial agonist
In vivo activity						
Insulin release	+	+	+	+	+	+
Appetite reduction	+	+	+	+	+	+
HbA1c reduction	+	+	+	+	+	+
Body weight reduction	+	+	+	?	?	+
CVD benefit	+	+	+	?	?	+

HbA1c, hemoglobin A1c; CVD, cardiovascular disease. NA, not active.